



## **Air-Flow separation above unsteady breaking waves**

Nicolas Reul, Hubert Branger, Jean-Paul Giovanangeli

### **► To cite this version:**

Nicolas Reul, Hubert Branger, Jean-Paul Giovanangeli. Air-Flow separation above unsteady breaking waves. *Physics of Fluids*, 1999, 11 (7), pp.1959-1961. <10.1063/1.870058>. <hal-00192471>

**HAL Id: hal-00192471**

**<https://hal.science/hal-00192471v1>**

Submitted on 26 Apr 2023

**HAL** is a multi-disciplinary open access archive for the deposit and dissemination of scientific research documents, whether they are published or not. The documents may come from teaching and research institutions in France or abroad, or from public or private research centers.

L'archive ouverte pluridisciplinaire **HAL**, est destinée au dépôt et à la diffusion de documents scientifiques de niveau recherche, publiés ou non, émanant des établissements d'enseignement et de recherche français ou étrangers, des laboratoires publics ou privés.



HAL Authorization

## Air flow separation over unsteady breaking waves

N. Reul, H. Branger, and J.-P. Giovanangeli

Citation: *Phys. Fluids* 11, 1959 (1999); doi: 10.1063/1.870058

View online: <http://dx.doi.org/10.1063/1.870058>

View Table of Contents: <http://pof.aip.org/resource/1/PHFLE6/v11/i7>

Published by the AIP Publishing LLC.

---

### Additional information on Phys. Fluids

Journal Homepage: <http://pof.aip.org/>

Journal Information: [http://pof.aip.org/about/about\\_the\\_journal](http://pof.aip.org/about/about_the_journal)

Top downloads: [http://pof.aip.org/features/most\\_downloaded](http://pof.aip.org/features/most_downloaded)

Information for Authors: <http://pof.aip.org/authors>

### ADVERTISEMENT



**Running in Circles Looking  
for the Best Science Job?**

**Search hundreds of exciting  
new jobs each month!**

<http://careers.physicstoday.org/jobs>

**physicstodayJOBS**



## Air flow separation over unsteady breaking waves

N. Reul,<sup>a)</sup> H. Branger, and J.-P. Giovanangeli

*Institut de Recherche Sur les Phénomènes Hors Equilibre, Laboratoire IOA, Case 903, 163, avenue de Luminy, 13288 Marseille, France*

(Received 28 April 1998; accepted 26 March 1999)

The evolution of the airflow instantaneous structure over an unsteady breaking wave propagating in a group is measured in detail using the digital particle image velocimetry technique. It is found that the boundary-layer over a breaking wave, the steepest in the group, separates at a point close to the sharp crest and reattaches in the front slope of the following wave. During breaking, the evolution of the turbulent vorticity is essentially unsteady and the recirculation zone of the separated flow takes the form of a large well-organized vortex. Links between the wave-crest geometry and geometrical features of the separation bubble have been established. © 1999 American Institute of Physics. [S1070-6631(99)01607-4]

One of the most debated open questions of small scale air-sea interaction is concerned with the role of breaking waves. Understanding of the air-flow dynamics above the breaking waves is of key importance for the parameterization of the momentum, mass and heat transfer between atmosphere and ocean. However, no realistic theoretical model of the phenomena has been yet developed due to the lack of direct observations of the air flow just above the water surface. Precise measurements of the velocity field in the close vicinity of a moving water surface that breaks up are indeed very difficult since breaking is an unsteady phenomenon, occurring intermittently, starting suddenly and evolving rapidly. This principal difficulty took two decades to be overcome. Banner & Melville<sup>1</sup> were the first to reveal that breaking or near-breaking induce air-flow separation over the waves. Their experiments, as well as those later performed by Banner,<sup>2</sup> aimed at establishing a *statistical* description of the air flow above the breaking waves. However, it is also of crucial importance to know the instantaneous structure of turbulence over breaking waves, particularly to improve existing models of sea-spray droplets production, entrainment, and evaporation.

The first attempt to describe the instantaneous features of the air flow was done by Kawai,<sup>3</sup> who clearly visualized separated air-flow patterns over short wind-waves. However, the limitations of his method did not allow Kawai to follow the evolution of the patterns and to resolve accurately the flow within the separation bubbles. Instantaneous velocity-shear measurements in the separated flow over wind waves were later performed by Kawamura & Toba.<sup>5</sup> While they detected a high-shear layer at the edge of the separation bubbles and deduced an *averaged* location of the reattachment point, their results were confined to point values of vorticity at a fixed level from the interface. In both experiments, the region of the flow extending from the free-surface to the separated shear-layer and the important reattachment area were not clearly identified. Moreover, the flow was only investigated over the so-called *micro-breaking* waves while typical wind waves are often breaking more intensively. The present work fills this gap. Using the new digital particle image velocimetry technique (DPIV), it provides, for various

levels of breaking intensity, a detailed quantified description of the *formation* and *evolution* of the air-flow patterns over a single propagating breaking wave.

The experiments reported here were performed in the small IRPHE-Luminy wind-wave facility.<sup>6</sup> The objective of these experiments was to examine the evolution of the air-flow characteristics over the water surface during the passage of an isolated breaking wave propagating in a group. At the upwind end of the tank, a vertically oscillating wedge wave-maker produced a frequency-modulated wave packet so that wave energy was focused at a predetermined time ( $\pm 10$  ms) and location ( $\pm 3$  cm) in the tank.<sup>7,8</sup> The coalescence of these waves under a moderate wind forcing with a free-stream value of  $U_o = 6 \text{ m.s}^{-1}$ , led to the formation of a 0.4 s period breaking wave, at approximately 5 m from the tank entrance. To avoid perturbations in the air-flow, the wedge-wave-maker was completely immersed in the water at the end of the group generation.

The instantaneous air-flow velocity field was obtained at the breaking region, using a cross-correlation DPIV technique similar to that described by Willert and Gharib.<sup>9</sup> The flow was seeded with  $8 \pm 5 \text{ } \mu\text{m}$  water droplets injected by a spray gun at the inlet of the flume. Two 12 mJ pulsed Nd:Yag laser generated a light beam at 532 nm which was turned into a light sheet about 1.5 mm thick through a series of optics and mirrors. This light sheet was directed from above the tank towards the water surface and slightly inclined at  $10^\circ$  from the vertical. It intersected with the water surface creating a well-defined line, parallel to the wind direction. A charge coupled device (CCD) camera then recorded images of the illuminated particles above the waves, viewing them from the side and looking down with an angle of  $10^\circ$  from the horizontal. The pulse separation between image pairs was  $100 \text{ } \mu\text{s}$  and the field of view was set to  $12.6 \times 9.3 \text{ cm}^2$ . This area was digitized at  $768 \times 484$  pixels,<sup>2</sup> and processed with interrogating window size of  $32 \times 32$  pixels<sup>2</sup> with 50% window overlap. The data processing results in a field measurement of  $47 \times 29$  velocity vectors and in a spatial wavelength resolution of  $0.26 \times 0.34 \text{ cm}^2$ . The optical property of the interface was used to provide the water surface profile coordinates<sup>10</sup> and the DPIV images were

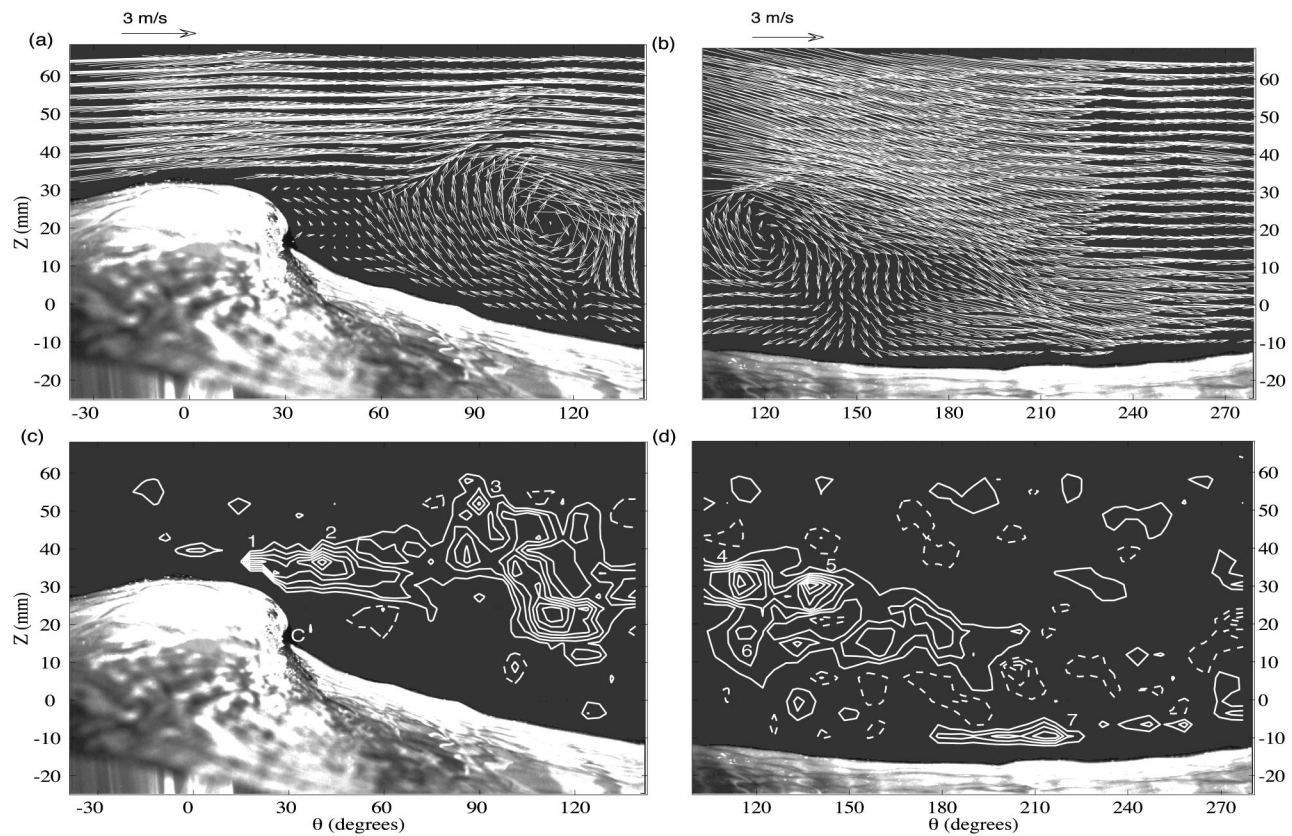


FIG. 1. (a) and (b): Air-flow instantaneous velocity distributions in the laboratory frame and (c) and (d): corresponding contours of constant positive (dashed lines) and negative (solid lines) vorticity over sections of a transient spilling breaking wave. (a) and (c) represent the flow over part of the breaker 135 ms after (b) and (d). Minimum and incremental levels of vorticity are both  $|\omega_{\min}| = \Delta\omega = 100 \text{ s}^{-1}$ .  $\theta$  is the wave phase relative to the crest and  $Z$  is the height relative to the mean water level in the plane of the light sheet.  $C$  is a convergence point at the water surface.

analyzed in the free-surface region using the method of Dabiri and Gharib.<sup>11</sup> The data acquisition process was synchronized with the signal sent to the wavemaker and triggered when the breaker crossed the camera field of view. Two image pairs of the illuminated particles over sections of the breaking wave were sequentially recorded with a time separation of 135 ms. The breaker wavelength  $\lambda$  was obtained from the imaging of the water surface and as a first approach, the velocity of the wave  $C_p$  was approximated from its period, using the linear dispersion relationship for deep gravity-waves.

Two key stages of the flow evolution over two wavelength-fractions of a typical spilling breaker ( $\lambda = 26.2 \text{ cm}$  and  $C_p = 0.64 \text{ m.s}^{-1}$ ) are illustrated by Fig. 1. As expected, the present experiments clearly reveal the existence of a separated-flow region downwind of a breaking crest and provide new features of its turbulence structure. A well-defined recirculating motion above the free surface thus extends from the trough region up to the crest of the wave. The maximum backflow in this zone is approximately 20% of  $U_o$  as is typical of “backward-facing” step separated flows<sup>12</sup> and is not a dead air-zone. The vorticity distributions clearly show that the separated-flow is bounded from above by a high-shear layer dominated by strongly localized coherent patches of negative vorticity (solid contours). Similarly to the flow over micro-breakers,<sup>4,5</sup> the shear layer seems to depart from the interface at a point where the slope of the free

surface exhibits an abrupt change. While the DPIV method is not resolving the flow at the interface but approximately 1 mm above it, at the larger scales, the flow appears to separate from the vicinity of the crest and *not* above the convergence point  $C$  (the latter is deduced from the known kinematical properties of breakers<sup>10,11</sup>). This suggests that multiple scales of the flow are involved in the separation process. The onset of separation may depend on the occurrence of a stagnation point at the interface but the diffusion of vorticity upwards in the direction normal to the interface is more likely controlled by the interplay between the adverse pressure gradient on the downwind side of the wave and the turbulence in the air flow. The separated flow over this spilling breaker is seen to reattach to the water surface in a region of high-shear, between  $\theta = 180^\circ$  and  $\theta = 220^\circ$ . The vorticity peak value of  $-542 \text{ s}^{-1}$  found at  $\theta = 215^\circ$  (point 7), is interpreted as the instantaneous reattachment point and is located closer to the crest than the average position found in previous studies. A new important characteristic parameter of the flow: the shedding frequency of small-scale vortices in the initial region of the separated-layer is determined. In the fixed frame, the convective velocity of the first rollers in the shear layer downwind of the crest (points 1 and 2) is approximately the average velocity across the shear layer, or  $\approx 2.1 \text{ m.s}^{-1}$ . The distance between their center is approximately 17 mm, resulting in a shedding frequency of  $(2.1 \text{ (m.s}^{-1})/0.017 \text{ m}) \approx 124 \text{ Hz}$ , which is of order 50 times greater than the wave

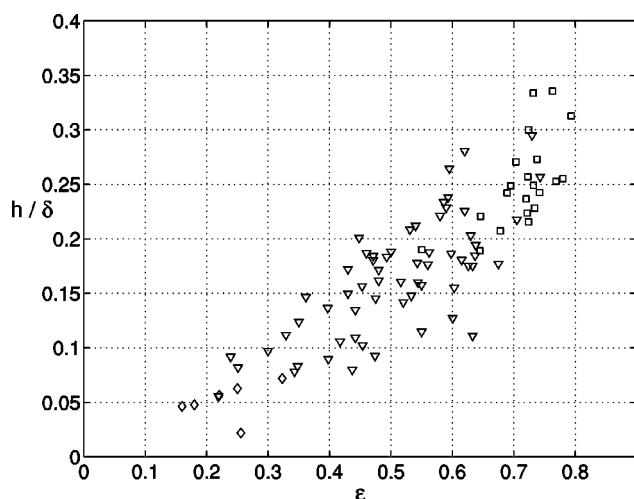


FIG. 2. Evolution of the separated layer characteristic height  $h$  over the first  $120^\circ$  phase angles of the breakers vs their crest front steepnesses. ( $\diamond$ : Incipient breaking,  $\nabla$ : Spilling breakers, and  $\square$ : Plunging breakers). The separated-layer thickness  $h$  is scaled by the boundary-layer thickness  $\delta$  [the height where  $U(z) = 0.99U_0$ ], measured to be equal to 8.2 cm at 5 m from the tank entrance.

frequency. Thus, the turbulent processes at separation are very fast compared to wave-period.

The main new result concerning this flow is that the central region of the separation bubble is not vorticity-free but exhibits a dynamically significant vortex. We traced the process of its formation and evolution. The curvature of the separation streamline (locus of negative vorticity maxima) and the distributions of coherent vorticity within the separated shear-layer evolved significantly within a small fraction of the wave period: e.g., in our particular example, the upper boundary of the layer in Fig. 1(d) exhibits two peak values of  $-749.8$  and  $-814 \text{ s}^{-1}$  (respectively, numbered 4 and 5) and a lower level of  $-378.6 \text{ s}^{-1}$  at the large scale vortex center (numbered 6); just 135 ms later the vorticity at the recirculating vortex center nearly doubled ( $-827.1 \text{ s}^{-1}$ ), while in the shear-layer (averaged over the points 1,2,3) decreased down to  $-584.1 \text{ s}^{-1}$ . This illustrates the formation of a roller-type motion in the form of a strong, large-scale vortex between the free-surface and the separated layer during the unsteady separation process. This vortex was convected with the phase-velocity  $C_p$  during the breaker propagation, since its core position in the frame of the wave remained constant (over  $\theta \approx 115^\circ$ ).

The flow structure was investigated over families of wave packets, systematically generated by varying their energy focusing point position and their initial steepness. The flow was thus captured over waves in a state ranging from incipient to fully evolved breaking and with breaking intensities ranging from slight spilling to violent plunging. We found that the appearance of the separation process is dependent on local properties of the waves but the spatial development of the separation bubbles is strongly linked with integral or large-scale characteristics of the wave form.

For each wave studied, the gradient of the surface was thus measured over an horizontal distance of approximately 3 mm, at equally spaced points along the wave profile.

Waves over which the flow separates always exhibit an abrupt change of slope downwind of the crest, with maximum local gradient values always greater than 0.7.

However, the vertical extent of the separated flow varied greatly as a function of the crest-shape. The crest-front steepness  $\epsilon$ ,<sup>12</sup> i.e., the ratio of the crest amplitude to the distance from the crest to the previous profile zero level crossing, was computed from the digitized wave profiles and used to characterize the instantaneous geometry of the breakers crests. The thickness of the separated-flow region downwind of the crest was parametrized by its mean height, defined as  $h = A/\lambda/3$ , where  $A$  is the area between the wave profile and the separation streamline over the first third of the wavelength. The dependence of  $h$  vs  $\epsilon$  is given in Fig. 2 and reveal that the instantaneous size of the separation bubble is controlled by the global geometry of the breaking crest: the steeper the crest, the higher the shear-layer above the water surface.

Thus, the breaking process serves as a strong intermittent source of turbulent vorticity in the air, which feeds the separated layer extending far downstream of the discontinuity at the crest. The evolution of the vorticity field suggests that the likely mechanism of the formation of the strong single vortex, attached to the wave between the free-surface and the separated layer, might be the re-entrainment of stress-bearing fluid from the outer part of the shear-layer. The established strong link of the size of the separation bubble with the crest geometry suggests that unsteadiness of the breaking process will result in intermittent growth and collapse of the large recirculating vortex, the fact of crucial importance for evaluating the dynamical significance of separation.

## ACKNOWLEDGMENTS

We are very grateful to V. Shrira for valuable comments. The work was supported by the French Direction des Recherches et Techniques (Grant No. 94.34.147).

<sup>a</sup>Electronic mail: nicolas@pollux.univ-mrs.fr

<sup>1</sup>M. L. Banner and W. K. Melville, "On the separation of air flow over water waves," *J. Fluid Mech.* **77**, 825 (1976).

<sup>2</sup>M. L. Banner, "The influence of wave breaking on the surface pressure distribution in wind wave interaction," *J. Fluid Mech.* **211**, 825 (1990).

<sup>3</sup>S. Kawai, "Structure of airflow separation over wind-wave crests," *Boundary-Layer Meteorol.* **23**, 503 (1982).

<sup>4</sup>H. Kawamura and Y. Toba, "Ordered motion in the turbulent boundary layer over wind waves," *J. Fluid Mech.* **197**, 105 (1988).

<sup>5</sup>M. Coantic and A. Favre, "Activities in, and preliminary results of, air-sea interactions research at IMST," *Adv. Geophys.* **16**, 391 (1974).

<sup>6</sup>R. J. Rapp and W. K. Melville, "Laboratory measurements of deep-water breaking waves," *Philos. Trans. R. Soc. London, Ser. A* **331**, 735 (1990).

<sup>7</sup>W. Jr. Pierson, M. A. Donelan, and W. H. Hui, "Linear and nonlinear propagation of water wave groups," *J. Geophys. Res.* **97**, 5607 (1992).

<sup>8</sup>C. E. Willert and M. Gharib, "Digital particle image velocimetry," *Exp. Fluids* **10**, 181 (1991).

<sup>9</sup>J. C. Lin and D. Rockwell, "Evolution of a quasi-steady breaking wave," *J. Fluid Mech.* **302**, 29 (1995).

<sup>10</sup>D. Dabiri and M. Gharib, "Experimental investigation of the vorticity generation within a spilling water wave," *J. Fluid Mech.* **330**, 113 (1997).

<sup>11</sup>P. Bonmarin, "Geometric properties of deep water breaking waves," *J. Fluid Mech.* **209**, 405 (1989).

<sup>12</sup>R. L. Simpson, "Turbulent boundary-layer separation," *Annu. Rev. Phys. Chem.* **21**, 205 (1989).